AerospaceEurope Conference2020
BORDEAUX, FRANCE | 25 - 28 FEBRUARY 2020
CEAS Council of European Aerospace Societies
HOSTED BY : 3AF Association Aéronautique et Astronautique de France

Paper: 621

STATION-KEEPING FOR HALO ORBITS USING A SOLAR SAIL WITH ONE-DEGREE-OF-FREEDOM ELECTRIC PROPULSION

Jia Huang[(1)], James D. Biggs[(2)], Naigang Cui[(3)]

[(1)(3)] Harbin Institute of Technology, Harbin, 150001, China, caep_huangjia@163.com, cui_naigang@163.com
[(1)] China Academy of Engineering Physics, Mianyang, 621999, China, caep_huangjia@163.com
[(2)] Politecnico di Milano, Milan, 20156, Italy, jamesdouglas.biggs@polimi.it

KEYWORDS: solar sail, solar electric propulsion, station-keeping, hybrid control, optical degradation

ABSTRACT:

This paper presents a scheme of a hybrid spacecraft which fuses a solar sail with a one-degree-of-freedom solar electric propulsion (SEP) fixed in the direction normal to the sail. This hybrid system significantly improves the available control acceleration in the normal direction of the sail and is more fuel-efficient than pure SEP spacecraft or hybrid solar sails with steerable SEP. The equations of motion of this hybrid system, with time-varying mass and lightness number, are described using the circular restricted three-body problem. The station-keeping is designed using an active disturbance rejection control method. The available control acceleration of this system is analyzed. Finally, simulations of station-keeping on a halo orbit are demonstrated taking into account injection errors and optical degradation. The results show that the presented hybrid system can significantly improve the robustness to injection errors and optical degradation.

1. INTRODUCTION

Halo orbits have been used for several deep-space missions [1] such as solar wind observation and communication relays. Classical halo orbits can be augmented using solar sail propulsion that enables completely new halo orbits which can extend the application of the classical halo orbits. Moreover, solar sail propulsion, which utilizes solar radiation pressure (SRP), is unlimited, completely green and renewable. However, solar sail halo orbits are inherently unstable and require three-degree-of-freedom station-keeping. A solar sail controls the direction of its SRP acceleration by varying its attitude. However, conventional solar sails cannot effectively control the magnitude of the SRP acceleration, such that the controllability of the motion in the normal direction of the sail is extremely weak.

Additional technologies can improve the controllability of the magnitude of the SRP acceleration such as introducing reflectivity control devices (RCDs), which have been demonstrated as an attitude control actuation system for JAXA's small solar power sail demonstrator "IKAROS" [2]. RCDs are able to control the magnitude of SRP acceleration by switching the optical properties between two states, for example, between specular reflection and diffuse reflection. This has enabled the possibility of more accurate orbit and attitude control [3]. However, the control acceleration provided by RCDs is highly constrained since the variation of the SRP acceleration due to the switch between specular reflection and diffuse reflection is significantly small relative to the total SRP acceleration. Moreover, only a small ratio of RCDs can be used on the sail surface due to their additional mass relative to the sail material. Therefore, when considering large uncertainties or disturbances, the station-keeping of a solar sail with RCDs could have poor performance or even completely fail. For example, [4] demonstrated that the station-keeping performance of an RCD solar sail can be significantly poor when taking into account the eccentricity of the Earth's orbit as a disturbance. Ref. [5] demonstrated that the station-keeping would fail when considering a long-term optical degradation.

To improve the available control acceleration in the normal direction of a solar sail, this paper proposes to combine a solar sail with a one-degree-of-freedom solar electric propulsion (SEP), where a SEP thruster is fixed along the normal direction of the sail and provides a propulsive force in both the positive and negative directions.

The idea of hybrid solar-sail/SEP has already been proposed for orbit design to enable new orbits that are impossible for pure solar sails and reduce the propellant consumption compared to spacecraft utilizing purely SEP [6, 7, 8, 9, 10, 11, 12]. In these applications, the SEP provides a part of the force to maintain the reference orbit, and the SEP thrusters are assumed to be steerable, that is, the direction and magnitude of the SEP thrust can be adjusted to provide three-degree-of-freedom control accelerations. However, this paper focuses on orbit control, where the reference halo orbit is designed without SEP, while the SEP is used to compensate for uncertainties and disturbances, but does not contribute to the reference orbit. This hybrid solar-sail/SEP system can significantly improve the available control acceleration in the normal direction of the sail compared to RCD solar sails and is more fuel-efficient than pure SEP spacecraft or hybrid solar sails with steerable SEP since it only needs to provide the control acceleration in the normal direction.

The equations of motion for this system are described by the Sun-Earth circular restricted three-body problem (CRTBP). The mass consumption is taken into account, and the sail lightness number is expressed as a function of the mass. In addition, an exponential optical degradation model [13, 14] is incorporated into the SRP acceleration model. The strategy proposed here uses an active disturbance rejection control (ADRC) [15, 16] coupled with an iterative process of control allocation for station-keeping.

Simulations of station-keeping on a halo orbit with this hybrid solar-sail/SEP system are demonstrated, taking into account large injection errors and optical degradation. The presented hybrid propulsion configuration is shown to significantly improve the robustness to injection errors and optical degradation, compared to solar sails with RCDs.

2. DYNAMICS OF THE SOLAR-SAIL/SEP SYSTEM

In this section, the equations of motion of the solar-sail/SEP system are described by the Sun-Earth CRTBP, where the mass and lightness number of the spacecraft are time-varying due to the propellant consumption, while a non-perfectly reflecting sail is considered, and the SEP thruster is fixed along the normal direction of the sail. In addition, the exponential optical degradation model proposed in [13, 14] is incorporated into the SRP acceleration model.

2.1 Equations of motion

The equations of motion are expressed in a rotating frame as shown in Fig. 1, where the origin is at the Sun-Earth barycenter, the *x*-axis points in the direction of the Earth, the *z*-axis is the axis of the rotation of the Sun-Earth system, and the *y*-axis completes the triad. In addition, the Sun-Earth distance, the frame's angular velocity, and the mass of the Sun-Earth system are normalized to unity.

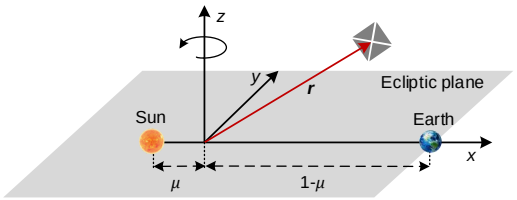

Figure 1: The rotating reference frame

The vectorial form of the equations of motion is given by

$$\boldsymbol{r}'' + 2\boldsymbol{\omega} \times \boldsymbol{r}' = \nabla U + \boldsymbol{a}_{\mathrm{SRP}} + \boldsymbol{a}_{\mathrm{SEP}} \tag{1}$$

where $\boldsymbol{r} = [x, y, z]^T$ is the non-dimensionalized position vector of the spacecraft, $\boldsymbol{\omega} = [0, 0, 1]^T$ is the non-dimensionalized angular velocity of the rotating frame, $\boldsymbol{a}_{\mathrm{SRP}}$ is the SRP acceleration, and $\boldsymbol{a}_{\mathrm{SEP}}$ is the SEP acceleration. The potential function U is given by

$$U = \frac{1}{2}(x^2 + y^2) + \frac{1-\mu}{r_1} + \frac{\mu}{r_2} \tag{2}$$

where $\mu = 3.04 \times 10^{-6}$ is the ratio of the Earth's mass to the total mass of the Sun-Earth system, and r_1 and r_2 are the non-dimensionalized distances from the spacecraft to the Sun and the Earth, respectively.

A non-perfectly reflecting SRP acceleration model is considered [13, 17], and the non-dimensionalized SRP acceleration $\boldsymbol{a}_{\mathrm{SRP}}$ is given by

$$\begin{aligned}\boldsymbol{a}_{\mathrm{SRP}} = \beta \frac{1-\mu}{2r_1^2} (\boldsymbol{s}\cdot\boldsymbol{n}) \Big\{ (1-s\rho)\boldsymbol{s} + \Big[2s\rho(\boldsymbol{s}\cdot\boldsymbol{n}) \\ + (1-s)\rho B_f + (1-\rho)\frac{\varepsilon_f B_f - \varepsilon_b B_b}{\varepsilon_f + \varepsilon_b} \Big] \boldsymbol{n} \Big\}\end{aligned} \tag{3}$$

where $\boldsymbol{n}$ is the unit vector normal to the sail, $\boldsymbol{s} = [x+\mu, y, z]^T / r_1$ is the unit vector of the Sun-spacecraft line, ρ is the reflection coefficient, s is the ratio of the specular reflection to the total reflection, ε_f and ε_b are the front and back emissivities, and B_f and B_b are the front and back non-Lambertian coefficients. The lightness number β varies with the mass of the spacecraft, that is

$$\beta = \beta_0 \frac{m_0}{m} \tag{4}$$

where m is the mass of the spacecraft in kilograms, and the subscript 0 indicates the initial time.

The unit vector $\boldsymbol{n}$ can be expressed in the rotating frame using two sail angles (a pitch angle γ and an azimuth angle δ), which are two control variables for the station-keeping, that is

$$\boldsymbol{n} = [\cos\gamma\cos\delta,\ \cos\gamma\sin\delta,\ \sin\gamma]^T \tag{5}$$

The non-dimensionalized SEP acceleration $\boldsymbol{a}_{\mathrm{SEP}}$, whose direction is along the sail normal, is given by

$$\boldsymbol{a}_{\mathrm{SEP}} = \frac{1}{\Omega^2 R_{12}} \frac{T}{m} \boldsymbol{n} \tag{6}$$

where T is the SEP thrust in Newtons, which is positive when its direction is in the same direction to the sail normal and negative when its direction is in the opposite direction to the sail normal. In addition, T is the other one control variable for the station-keeping. The term $\Omega^2 R_{12}$ is used to non-dimensionalize the acceleration, where $\Omega = 1.991 \times 10^{-7}$ rad/s is the average angular velocity of the rotating frame, and $R_{12} = 1.496 \times 10^{11}$ m is the average Sun-Earth distance.

The mass consumption rate is given by

$$\dot{m} = \frac{T}{I_{sp} g_0} \tag{7}$$

where I_{sp} is the specific impulse in seconds, and $g_0 = 9.80665$ m/s^2 is the normal gravitational acceleration.

We define $\boldsymbol{a}$ the sum of $\boldsymbol{a}_{\mathrm{SRP}}$ and $\boldsymbol{a}_{\mathrm{SEP}}$, and the control vector $\boldsymbol{u} = [\gamma, \delta, T]^T$. Therefore, $\boldsymbol{a}$ is a function of $\boldsymbol{u}$, that is

$$\boldsymbol{a} = \boldsymbol{a}_{\mathrm{SRP}} + \boldsymbol{a}_{\mathrm{SEP}} = \boldsymbol{g}(\boldsymbol{u}) \tag{8}$$

where, if $\boldsymbol{a}$ is known, $\boldsymbol{u}$ can be obtained by solving Eq. 8 using a nonlinear method.

The same values for I_{sp}, m_0, and the maximum SEP thrust $T_{\max}$ as in [6] are used, that is, $I_{sp} = 3200$ s, $m_0 = 1000$ kg, and $T_{\max} = 0.15$ N. The initial lightness number β_0 is set to 0.05, which is a typical value for early solar storm warnings and used in [5, 6, 7, 18, 19]. In addition, the values of the optical coefficients are taken from [20], that is, $\rho = 0.91$, $s = 0.89$, $\varepsilon_f = 0.025$, $\varepsilon_b = 0.27$, $B_f = 0.79$, and $B_b = 0.67$.

2.2 Optical degradation model

The exponential optical degradation model, which takes into account the solar radiation dose (SRD) [13, 14], is considered, that is

$$\frac{p(t)}{p_0} = \begin{cases} (1 + de^{-\lambda\Sigma(t)})/(1+d), & \text{for } p \in \{\rho,\ s\} \\ 1 + d(1 - e^{-\lambda\Sigma(t)}), & \text{for } p = \varepsilon_f \\ 1, & \text{for } p \in \{\varepsilon_b, B_f,\ B_b\} \end{cases} \tag{9}$$

where p denotes a generic optical coefficient. The parameter d is a degradation factor parameterizing the maximum variation in p, and $\lambda = \ln 2/\hat{\Sigma}$ is a degradation constant parameterizing the rate of degradation, where $\hat{\Sigma}$ is the relative SRD when $p = (p_0 + p_\infty)/2$, where the subscripts 0 and ∞ denote the initial time and the moment after infinite time, respectively. Finally, $\Sigma(t)$ is the relative SRD, which can be computed by

$$\dot{\Sigma}(t) = r_0^2 \cos\alpha / r^2 \tag{10}$$

where $r_0 = 1$ AU is the distance between the Sun and the Earth, r is the distance between the Sun and the spacecraft, and α is the angle between the sail normal and the Sun-spacecraft line.

At 1 AU from the Sun along the Sun-Earth line and with $d = 0.05$ and $\hat{\Sigma} = 5$, the variations of the optical coefficients with time are shown in Fig. 2.

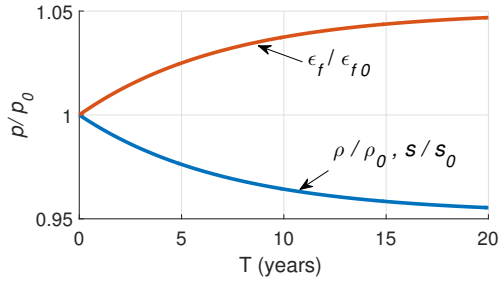

Figure 2: Variation of the optical coefficients with time

2.3 Control acceleration analysis

In this subsection, a simple example is used to analyze the available control acceleration of the presented solar-sail/SEP system, compared to RCD solar sails. A scenario is assumed, where a perfectly reflecting solar sail with $\beta = 0.05$ is at the point 0.98 AU far from the Sun on the Sun-Earth line, and the azimuth angle $\delta = 0$ is constant, that is, only considering the dynamics in the x-z plane. In this case, the SRP acceleration model reduces to

$$\boldsymbol{a}_{\mathrm{SRP}} = \beta \frac{1-\mu}{r_1^2} \cos^2\gamma [\cos\gamma,\ 0,\ \sin\gamma]^T \tag{11}$$

Obviously, when γ = 0, the SRP acceleration reaches its maximum value and is directed along the *x*-direction, that is

$$\boldsymbol{a}_{\mathrm{SRP}} = a_{\max}[1,\ 0,\ 0]^T = \beta\frac{1-\mu}{r_1^2}[1,\ 0,\ 0]^T \qquad (12)$$

where the maximum SRP acceleration $a_{\max}$ = 0.3087 mm/s^2. This state is considered as the reference state of the solar sail, and the control acceleration is defined as the deviation from the reference acceleration, i.e., $\Delta\boldsymbol{a} = \boldsymbol{a} - \boldsymbol{a}_e$, where the subscript *e* indicates the reference state.

First, the maximum available control acceleration in the *z*-direction can be obtained by solving Eq. 13 for γ, which is then substituted into Eq. 11.

$$\frac{\partial \boldsymbol{a}_{\mathrm{SRP},z}}{\partial\gamma} = \beta\frac{1-\mu}{r_1^2}(1-3\sin^2\gamma)\cos\gamma = 0 \qquad (13)$$

where the subscript *z* and the following subscripts *x* and *y* denote the components in the corresponding directions, respectively. It can be calculated that the maximum available control acceleration in the *z*-direction $\Delta\boldsymbol{a}_{\max,z}$ = 0.385$a_{\max}$, when γ = 35.26° and δ = 0°. The maximum available control acceleration in the *y*-direction can be obtained in the same way, that is, $\Delta\boldsymbol{a}_{\max,y}$ = 0.385$a_{\max}$, when δ = 35.26° and γ = 0°.

Then, the focus is placed on the maximum available control acceleration in the *x*-direction $\Delta\boldsymbol{a}_{\max,x}$. For the reference state, it can be seen that the SRP acceleration in the *x*-direction has reached its maximum value. Therefore, it is impossible to obtain positive control acceleration in the *x*-direction by varying the sail angles only. Thus, additional control technologies should be incorporated, such as RCDs or SEP.

An RCD can switch between a specular state, in which most of the photons are specularly reflected, and a diffuse state, in which most of the photons are diffusely reflected. For the diffuse state, it is assumed that all the specular reflection transforms to diffuse reflection. The optical properties of the sail surface without RCDs are assumed to be the same as those of the RCDs in the specular state. With these assumptions, the SRP acceleration model of an RCD solar sail in the reference state can be given by

$$\boldsymbol{a}_{\mathrm{SRP}} = \beta K\frac{1-\mu}{r_1^2}[1,\ 0,\ 0]^T \qquad (14)$$

$$K = \frac{1}{2}\Big[1 + s\rho(1-\sigma)(1-B_f) + \rho B_f + (1-\rho)\frac{\varepsilon_f B_f - \varepsilon_b B_b}{\varepsilon_f + \varepsilon_b}\Big] \qquad (15)$$

where the RCD ratio σ is defined as the ratio of the area of the RCDs in the diffuse state to the total sail area. According to Eqs. 14-15, $\boldsymbol{a}_{\mathrm{SRP},x}$ is a function of σ, that is, $\boldsymbol{a}_{\mathrm{SRP},x}$ can be controlled by adjusting σ. The maximum available control acceleration of the RCD solar sail in the *x*-direction can be given as

$$\Delta\boldsymbol{a}_{\max,x} = \boldsymbol{a}_{\mathrm{SRP},x}(\sigma_{\max}) - \boldsymbol{a}_{\mathrm{SRP},x}(\sigma_e) \qquad (16)$$

where $\sigma_{\max}$ is the maximum RCD ratio, equal to the ratio of the total RCD area to the total sail area, and σ_e is the nominal RCD ratio corresponding to the reference orbit. Usually, σ_e is set to a half of $\sigma_{\max}$ such that the RCDs can provide equal maximum positive and negative control accelerations. Considering three solar sails with different coverage rates of RCDs, i.e., $\sigma_{\max}$ = 0.1, 0.5, and 1, respectively, the corresponding maximum control accelerations $\Delta\boldsymbol{a}_{\max,x}$ are 0.004$a_{\max}$, 0.021$a_{\max}$, and 0.043$a_{\max}$, respectively, calculated using Eq. 16. Therefore, $\Delta\boldsymbol{a}_{\max,x}$ provided by the RCDs is significant smaller than $\Delta\boldsymbol{a}_{\max,y}$ and $\Delta\boldsymbol{a}_{\max,z}$. In contrast, the maximum control acceleration provided by the SEP with the parameters set in Section 2.1 (m_0 = 1000 kg, $T_{\max}$ = 0.15 N) is 0.485$a_{\max}$, which is comparable to $\Delta\boldsymbol{a}_{\max,y}$ and $\Delta\boldsymbol{a}_{\max,z}$.

Tab. 1 summarizes the maximum control accelerations in the three directions for the RCD solar sails and the solar-sail/SEP system. For the RCD solar sails, $\boldsymbol{a}_{\max,x}$ is significantly smaller than $\boldsymbol{a}_{\max,y}$ and $\boldsymbol{a}_{\max,z}$, such that the overall control capability is limited by $\boldsymbol{a}_{\max,x}$, while the solar-sail/SEP system can provide balanced control accelerations in the three directions.

3. STATION-KEEPING CONTROL DESIGN

In this paper, an ADRC based control scheme presented in [5] is used to design the station-keeping, in which an ADRC control law is used to obtain the required control acceleration $\Delta\boldsymbol{a}$, and then, the Newton's method is used to map $\Delta\boldsymbol{a}$ to the control vector $\boldsymbol{u}$.

3.1 System model for control

The equations of motion in Eq. 1 can be transformed into the following form

$$\begin{aligned}\dot{\boldsymbol{r}} &= \boldsymbol{v}\\ \dot{\boldsymbol{v}} &= \boldsymbol{f}(\boldsymbol{r},\boldsymbol{v}) + \boldsymbol{a}\end{aligned} \qquad (17)$$

where $\boldsymbol{v} = [v_x, v_y, v_z]^T$ is the velocity vector, $\boldsymbol{f} = \nabla U - 2\boldsymbol{\omega}\times\boldsymbol{v}$ is the nonlinear dynamics, and $\boldsymbol{a} = \boldsymbol{a}_{\mathrm{SRP}} + \boldsymbol{a}_{\mathrm{SEP}}$.

Table 1: Maximum control accelerations in the three directions

	y-direction	*z*-direction	*x*-direction			
	$\delta = 35.26^\circ$	$\gamma = 35.26^\circ$	RCD solar sails			solar-sail/SEP
	$\gamma = 0^\circ$	$\delta = 0^\circ$	$\sigma_{max} = 0.1$	$\sigma_{max} = 0.5$	$\sigma_{max} = 1$	$m_0 = 1000$kg, $T_{max} = 0.15$N
$\Delta\boldsymbol{a}_{max}$	$0.385a_{max}$	$0.385a_{max}$	$0.004a_{max}$	$0.021a_{max}$	$0.043a_{max}$	$0.485a_{max}$

The deviation equations of motion relative to the reference orbit are used as the system model for control design, that is

$$\begin{aligned} \Delta\dot{\boldsymbol{r}} &= \Delta\boldsymbol{v} \\ \Delta\dot{\boldsymbol{v}} &= \Delta\boldsymbol{f}(\boldsymbol{r},\boldsymbol{v}) + \boldsymbol{d} + \Delta\boldsymbol{a} \end{aligned} \tag{18}$$

where $\Delta\boldsymbol{r} = \boldsymbol{r} - \boldsymbol{r}_e$, $\Delta\boldsymbol{v} = \boldsymbol{v} - \boldsymbol{v}_e$, $\Delta\boldsymbol{f} = \boldsymbol{f}(\boldsymbol{r},\boldsymbol{v}) - \boldsymbol{f}(\boldsymbol{r}_e,\boldsymbol{v}_e)$, and $\Delta\boldsymbol{a} = \boldsymbol{a} - \boldsymbol{a}_e$ are the deviations from the reference orbit, whereas $\boldsymbol{d}$ is the disturbance due to the errors in the optical properties (hereinafter called the optical error). Here the nominal acceleration $\boldsymbol{a}_e$ is only due to the SRP acceleration.

The total disturbance $\boldsymbol{w}$ is given by $\boldsymbol{w} = \Delta\boldsymbol{f} + \boldsymbol{d}$, so that Eq. 18 can be written as

$$\begin{aligned} \Delta\dot{\boldsymbol{r}} &= \Delta\boldsymbol{v} \\ \Delta\dot{\boldsymbol{v}} &= \boldsymbol{w} + \Delta\boldsymbol{a} \end{aligned} \tag{19}$$

where $\Delta\boldsymbol{r}$ and $\Delta\boldsymbol{v}$ are the states, $\Delta\boldsymbol{a}$ is the control variable, and $\boldsymbol{w}$ is the disturbance. The basic concept of ADRC is to estimate $\boldsymbol{w}$ using an extended state observer (ESO), and then compensate for it in the control input, so that the system of Eq. 19 reduces to a linear cascade integral system.

For the control to be feasible, the magnitude of the disturbance $|\boldsymbol{w}| = |\Delta\boldsymbol{f} + \boldsymbol{d}|$ must be smaller than the maximum available control acceleration $\Delta\boldsymbol{a}_{max}$. In addition, $\Delta\boldsymbol{f}$ depends on the orbit error relative to the reference orbit, while $\boldsymbol{d}$ depends on the optical errors. Therefore, when large orbit errors or optical errors arise, the station-keeping could fail if $\Delta\boldsymbol{a}_{max}$ is not large enough.

3.2 ADRC based control scheme

The ADRC based control scheme consists of a nonlinear ESO, a nonlinear time-optimal feedback law, and an iterative algorithm for solving nonlinear equations [5]. The control laws for the three channels (*x*, *y*, and *z*) are designed independently, and the coupled items are viewed as a disturbance.

Taking the *x* channel as an example, the nonlinear ESO is given in a discrete form

$$\begin{aligned} e_k &= \Delta\hat{x}_k - \Delta x_k \\ \Delta\hat{x}_{k+1} &= \Delta\hat{x}_k + h(\Delta\hat{v}_{x,k} - \beta_1 e_k) \\ \Delta\hat{v}_{x,k+1} &= \Delta\hat{v}_{x,k} + h\,(\Delta\hat{w}_{x,k} - \beta_2 \mathrm{fal}\,(e_k, 1/2, h) + \Delta a_x) \\ \Delta\hat{w}_{x,k+1} &= \Delta\hat{w}_{x,k} + h\,(-\beta_3 \mathrm{fal}\,(e_k, 1/4, h)) \end{aligned} \tag{20}$$

where h is the control period, $\Delta\hat{x}$ and $\Delta\hat{v}_x$ are the estimated deviations of position and velocity from the reference orbit, $\hat{w}_x$ is the estimated disturbance, and β_i (i=1, 2, 3) are the observer gains. The function fal() is defined in [15, 16], that is

$$\mathrm{fal}(\varepsilon,\tau,\eta) = \begin{cases} \dfrac{\varepsilon}{\eta^{1-\tau}}, & |\varepsilon| \le \eta \\ |\varepsilon|^{\tau}\mathrm{sign}(\varepsilon), & |\varepsilon| > \eta \end{cases} \tag{21}$$

The required control acceleration is given by

$$\Delta a_x = \Delta a_{1,x} - \hat{w}_x \tag{22}$$

with

$$\Delta a_{1,x} = \mathrm{fhan}(\Delta\hat{x}, c_x\Delta\hat{v}_x, \bar{r}_x, \bar{h}_x) \tag{23}$$

where $\bar{r}_x$ is the maximum control acceleration, and c_x and $\bar{h}_x$ are the two control parameters. The function fhan() is a nonlinear time-optimal feedback law, which is defined in [15, 16], that is

$$\begin{cases} D = \bar{r}\bar{h}^2,\ A_0 = \bar{h}x_2,\ Y = x_1 + A_0 \\ A_1 = \sqrt{D(D + 8|Y|)},\ A_2 = A_0 + \mathrm{sign}(Y)(A_1 - D)/2 \\ s_y = [\mathrm{sign}(Y + D) - \mathrm{sign}(Y - D)]/2 \\ A = (A_0 + Y - A_2)s_y + A_2 \\ s_a = [\mathrm{sign}(A + D) - \mathrm{sign}(A - D)]/2 \\ \mathrm{fhan}(x_1, x_2, \bar{r}, \bar{h}) = -\bar{r}\,[A/D - \mathrm{sign}(A)]\,s_a - \bar{r}\,\mathrm{sign}(A) \end{cases} \tag{24}$$

Then, the sum of $\boldsymbol{a}_{SRP}$ and $\boldsymbol{a}_{SEP}$ is given by $\boldsymbol{a} = \boldsymbol{a}_e + \Delta\boldsymbol{a}$, and the control vector $\boldsymbol{u}$ can be obtained by solving the nonlinear system of Eq. 8, which is equivalent to solving for the roots of Eq. 25.

$$\boldsymbol{F} = \boldsymbol{a} - \boldsymbol{g}(\boldsymbol{u}) = \boldsymbol{0} \tag{25}$$

The most common algorithm to solve this problem is the Newton's method, that is

$$\boldsymbol{u}_{k+1} = \boldsymbol{u}_k - (\boldsymbol{J}(\boldsymbol{u}_k))^{-1}\boldsymbol{F}(\boldsymbol{u}_k) \tag{26}$$

where $\boldsymbol{J}$ is the Jacobian matrix given by

$$\boldsymbol{J}(\boldsymbol{u}_k) = \left[\begin{array}{ccc} \frac{\partial F_1}{\partial u_1} & \frac{\partial F_1}{\partial u_2} & \frac{\partial F_1}{\partial u_3} \\ \frac{\partial F_2}{\partial u_1} & \frac{\partial F_2}{\partial u_2} & \frac{\partial F_2}{\partial u_3} \\ \frac{\partial F_3}{\partial u_1} & \frac{\partial F_3}{\partial u_2} & \frac{\partial F_3}{\partial u_3} \end{array}\right]_{t=t_k} \tag{27}$$

where F_i (i=1, 2, 3) and u_i (i=1, 2, 3) are the components of $\boldsymbol{F}$ and $\boldsymbol{u}$, respectively.

The nominal value for $\boldsymbol{u}_e$ is used as the initial guess for the iteration of Eq. 26.

Fig. 3 shows the flow chart of the control loop of the ADRC station-keeping.

4. NUMERICAL SIMULATION

In this paper, a typical halo orbit for early solar storm warnings [5], with the amplitude of 0.002 AU in the z-direction and around the artificial equilibrium point 0.98 AU far from the Sun on the Sun-Earth line, is used as the reference orbit, as shown in Fig. 4. The sail normal is directed along the Sun-spacecraft line in the reference state. The initial states of the reference orbit is

$$\begin{cases} x_0 = 0.975240874297760, \\ z_0 = -0.00213808168231298, \\ v_{y0} = 0.0135800625909357, \\ y_0 = 0,\ z_0 = 0,\ v_{x0} = 0,\ v_{z0} = 0 \end{cases} \tag{28}$$

As mentioned in Section 3.1, the necessary condition for effective station-keeping is that the total disturbance $\boldsymbol{w} = \Delta\boldsymbol{f} + \boldsymbol{d}$ is smaller than the maximum available control acceleration $\Delta\boldsymbol{a}_{\max}$. In addition, $\Delta\boldsymbol{f}$ and $\boldsymbol{d}$ depend on the orbit error and the optical errors, respectively. In this section, simulations are undertaken to analyze the station-keeping performances in the presence of large injection errors and optical degradation.

To demonstrate the improvement relative to RCD solar sails, an analysis is performed first to demonstrate the maximum orbit error and optical errors an RCD solar sail can overcome. Since the maximum control acceleration $\Delta\boldsymbol{a}_{\max,x}$ of an RCD solar sail is significantly smaller than its $\Delta\boldsymbol{a}_{\max,y}$ and $\Delta\boldsymbol{a}_{\max,z}$, the analysis can only focus on the x-direction. Therefore, the necessary condition for effective station-keeping can be given as $|\boldsymbol{w}_x| < \Delta\boldsymbol{a}_{\max,x}$. To satisfy this condition, according to the values of $\Delta\boldsymbol{a}_{\max,x}$ of the three solar sails with different coverage rates of RCDs in Tab. 1, the maximum allowable orbit error and optical errors can be calculated, as shown in Tab. 2, where $r_{\max}$ and $v_{\max}$ denote the maximum errors of position and velocity in the three directions, respectively, and $d_{\max}$ is the maximum degradation factor in Eq. 9. These three factors are taken into account separately in Tab. 2.

The data in Tab. 2 are optimistic since $\Delta\boldsymbol{a}_{\max,x}$ is not only used to compensate for the disturbance $\boldsymbol{w}_x$ but also the variation of acceleration due to the change of the sail angles and other uncertainties, such as the estimation error of $\boldsymbol{w}_x$. Therefore, the condition $|\boldsymbol{w}_x| < \Delta\boldsymbol{a}_{\max,x}$ is only a necessary condition but not sufficient condition for effective station-keeping. However, it can be seen that the maximum allowable orbit errors and optical errors are significantly limited.

For the presented solar-sail/SEP system, the separate maximum available control accelerations in the x, y, and z directions are 0.150 mm/s^2, 0.119 mm/s^2, and 0.119 mm/s^2, respectively (see Tab. 1). However, the control accelerations in the three directions cannot reach their maximum values simultaneously since they are coupled. For example, the control acceleration in the z-direction can reach its maximum value, i.e. $0.385a_{\max}$, when $\gamma = 35.26°$ and $\delta = 0°$. However, in this case, the SRP acceleration in the x-direction reduces to $0.54a_{\max}$. Therefore, in the simulations, the maximum control accelerations in the three directions are limited to 0.092 mm/s^2 according to the simulation results, such that comparable control accelerations in the three directions can be obtained simultaneously. The control parameters are set as those given in [5], that is, h=0.001, $c_i = 1$, and $\bar{h}_i = 0.005$ (i = x, y, z).

A large number of simulations with different injection errors have been performed, and the results show that the solar-sail/SEP system, using the presented ADRC based station-keeping control, is able to overcome initial position errors of up to 1.06×10^6 km (see Fig. 5) or velocity errors of up to 216.5 m/s (see Fig. 6) in the three directions simultaneously, at the cost of propellant consumptions of 11.9 kg and 22.3 kg, respectively.

When considering an optical degradation, the critical problem is not the maximum SRP acceleration error due to the degradation, since the SEP can provide a control acceleration of $0.485a_{\max}$ (see Tab. 1), such that even the reflection coefficient degrades to 10% of its initial value, the SEP still can provide enough control acceleration to compensate for it. However, when an optical degradation exists, the SEP needs to compensate for the SRP acceleration error continuously, which leads to continuous propellant consumption. For example, setting the degradation parameters as d = 0.43 and λ = 0.1386, which implies that the reflection

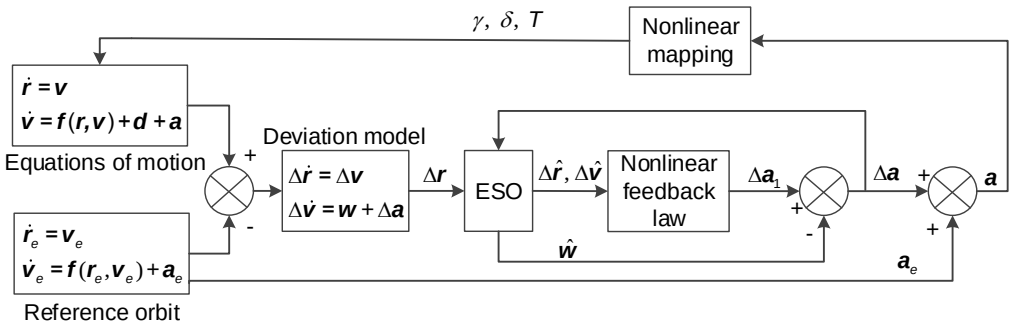

Figure 3: Control loop of the ADRC station-keeping

Table 2: Maximum allowable orbit errors and optical errors for RCD solar sails

	Three RCD solar sails		
	σ_{max} = 0.1	σ_{max} = 0.5	σ_{max} = 1
$\Delta \boldsymbol{a}_{max,x}$, mm/s^2	0.0013	0.0065	0.013
r_{max}, km	9604	47124	95982
v_{max}, m/s	3.3	16.4	33.3
d_{max}	0.0056	0.028	0.06

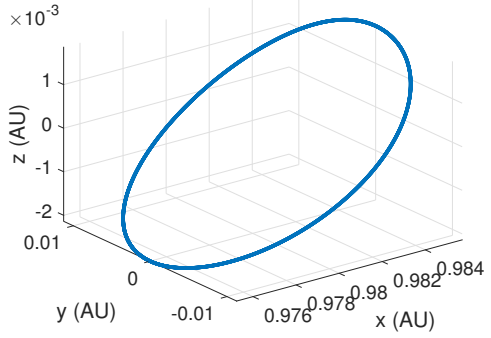

Figure 4: Reference orbit

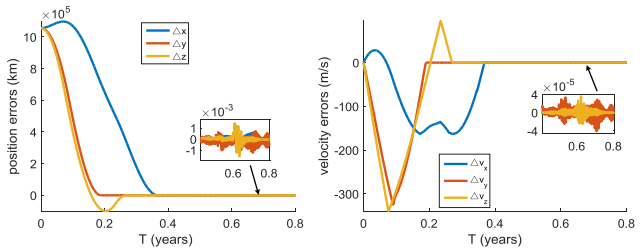

(a) Position errors and velocity errors

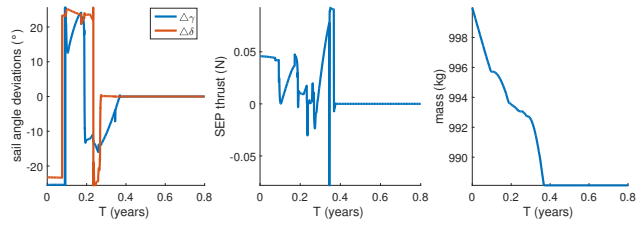

(b) Control variables and mass

Figure 5: Control results with maximum initial position errors

coefficient will degrade to 85% of its initial value in about 2 years and 70% of its initial value (the maximum degradation) asymptotically, the simulation results are demonstrated over a period of 10 years, as shown in Fig. 7. In the second subfigure of Fig. 7b, the SEP thrust increases exponentially in the first 5 years to compensate for the increasing optical degradation. In the left 5 years, the optical degradation has reached close to its maximum (see Fig. 7c), so that the SEP thrust starts to decrease as the mass decreases. In addition, 418 kg propellant has been consumed in this period.

5. CONCLUSION

This paper presents a hybrid solar-sail/SEP scheme which combines a solar sail with a one-degree-of-freedom solar electric propulsion (SEP) fixed along the normal direction of the sail. This hybrid system can significantly improve the available control acceleration in the normal direction

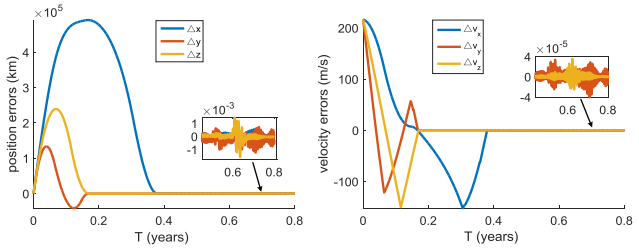

(a) Position errors and velocity errors

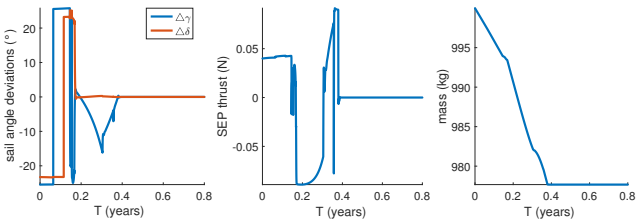

(b) Control variables and mass

Figure 6: Control results with maximum initial velocity errors

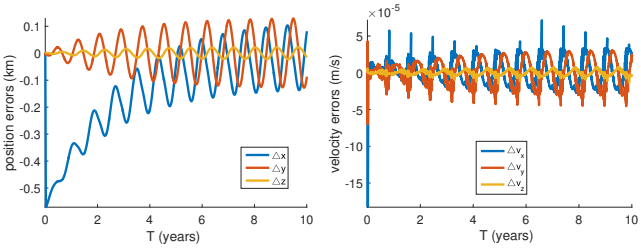

(a) Position errors and velocity errors

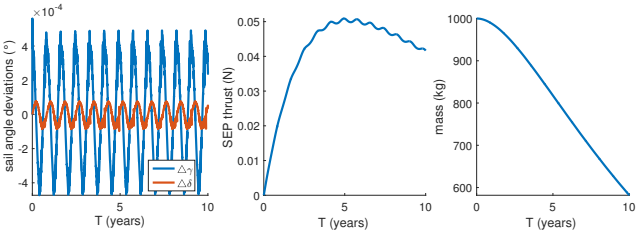

(b) Control variables and mass

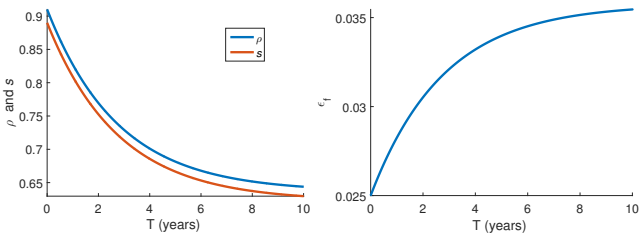

(c) Variations of the optical coefficients

Figure 7: Control results with optical degradation

of the solar sail, while it is more fuel-efficient than purely using SEP. The equations of motion of this hybrid system, with time-varying mass and lightness number of the sail, are described by the circular restricted three-body problem (CRTBP), and an exponential optical degradation model is incorporated into the solar radiation acceleration model. Furthermore, the station-keeping is designed using an active disturbance rejection control (ADRC) coupled with an iterative process of control allocation. The maximum control accelerations of this hybrid system are analyzed and compared to those of three typical solar sails with different amounts of reflectivity control devices (RCDs). The results show that the available control accelerations in the normal direction of the RCD solar sails are significantly smaller than those in the other two directions, while the solar-sail/SEP system can provide comparable control accelerations in the three directions. Finally, simulations of station-keeping on a typical halo orbit are demonstrated taking into account injection errors and optical degradations. The results show that the presented solar-sail/SEP system can significantly improve the robustness to injection errors and optical degradation compared to the RCD solar sails, at the cost of affordable propellant consumption.

REFERENCES

[1] M. Shirobokov, S. Trofimov, and M. Ovchinnikov. Survey of station-keeping techniques for libration point orbits. *J. Guid. Control Dyn.*, 40(5):1085–1105, 2017.

[2] R. Funase, Y. Shirasawa, Y. Mimasu, O. Mori, Y. Tsuda, T. Saiki, and J. Kawaguchi. On-orbit verification of fuel-free attitude control system for spinning solar sail utilizing solar radiation pressure. *Adv. Space Res.*, 48(11):1740–1746, 2011.

[3] J.D Biggs and A. Negri. Orbit-attitude control in a circular restricted three-body problem using distributed reflectivity devices. *J. Guid. Control Dyn.*, 42(12):2712–2721, 2019.

[4] J. Huang, J.D. Biggs, and N. Cui. Families of halo orbits in the elliptic restricted three-body problem for a solar sail with reflectivity control devices. *Adv. Space Res.*, 65(3):1070–1082, 2020.

[5] J. Huang, J.D. Biggs, Bai Y., and N. Cui. Integrated guidance and control for solar sail

station-keeping with optical degradation. *Adv. Space Res.*, 2020. (in press).

[6] M. Ceriotti and C.R. McInnes. Hybrid solar sail and solar electric propulsion for novel earth observation missions. *Acta Astronaut.*, 69(9-10):809–821, 2011.

[7] M. Ceriotti and C.R. McInnes. Systems design of a hybrid sail pole-sitter. *Adv. Space Res.*, 48(11):1754–1762, 2011.

[8] G. Mengali and A.A. Quarta. Trajectory design with hybrid low-thrust propulsion system. *J. Guid. Control Dyn.*, 30(2):419–426, 2007.

[9] J. Heiligers, M. Ceriotti, C.R. McInnes, and J.D. Biggs. Displaced geostationary orbit design using hybrid sail propulsion. *J. Guid. Control Dyn.*, 34(6):1852–1866, 2011.

[10] S. Gong, J. Li, and F. Jiang. Interplanetary trajectory design for a hybrid propulsion system. *Aerosp. Sci. Technol.*, 45:104–113, 2015.

[11] P. Anderson and M. Macdonald. Static, highly elliptical orbits using hybrid low-thrust propulsion. *J. Guid. Control Dyn.*, 36(3):870–880, 2013.

[12] S. Baig and C.R. McInnes. Artificial three-body equilibria for hybrid low-thrust propulsion. *J. Guid. Control Dyn.*, 31(6):1644–1655, 2008.

[13] B. Dachwald, G. Mengali, A.A. Quarta, and M. Macdonald. Parametric model and optimal control of solar sails with optical degradation. *J. Guid. Control Dyn.*, 29(5):1170–1178, 2006.

[14] B. Dachwald, M. Macdonald, C.R. McInnes, G. Mengali, and A.A. Quarta. Impact of optical degradation on solar sail mission performance. *J. Spacecraft Rockets*, 44(4):740–749, 2007.

[15] J. Han. From PID to active disturbance rejection control. *IEEE T. Ind. Electron.*, 56(3):900–906, 2009.

[16] J. Han. *Active Disturbance Rejection Control Technique: the Technique for Estimating and Compensating the Uncertainties*. National Defense Industry Press, Beijing, China, 2008. (in Chinese).

[17] C.R. McInnes. *Solar sailing: technology, dynamics and mission applications*. Springer and Praxis, Chichester, UK, 1999.

[18] J.D. Biggs, C.R. McInnes, and T. Waters. Control of solar sail periodic orbits in the elliptic three-body problem. *J. Guid. Control Dyn.*, 32(1):318–320, 2009.

[19] J.D. Biggs and C.R. McInnes. Solar sail formation flying for deep-space remote sensing. *J. Spacecraft Rockets*, 46(3):670–678, 2009.

[20] A. Heaton, N. Ahmad, and K. Miller. Near earth asteroid scout solar sail thrust and torque model. In *Proceedings of the 4th International Symposium on Solar Sailing*, Kyoto, Japan, 2017.